Cancer Letters 461 (2019) 90–101

Contents lists available at ScienceDirect

Cancer Letters

journal homepage: www.elsevier.com/locate/canlet

Original Articles

Pro-differentiating and radiosensitizing effects of inhibiting HDACs by PXD-101 (Belinostat) in *in vitro* and *in vivo* models of human rhabdomyosarcoma cell lines

Francesco Marampon[a,*,1], Valentina Di Nisio[b,1], Ilaria Pietrantoni[c], Francesco Petragnano[c], Irene Fasciani[c], Bianca Maria Scicchitano[d], Carmela Ciccarelli[c], Giovanni Luca Gravina[c], Claudio Festuccia[c], Andrea Del Fattore[e], Mario Tombolini[f], Francesca De Felice[a], Daniela Musio[a], Sandra Cecconi[b], Paolo Tini[g,h], Marta Maddalo[i], Silvia Codenotti[j], Alessandro Fanzani[j], Antonella Polimeni[k], Roberto Maggio[c,1], Vincenzo Tombolini[a,1]

[a] Department of Radiology, Radiotherapy, Oncology and Anatomopathology, Policlinico Umberto I, "Sapienza" University of Rome, Rome, Italy
[b] Department of Life, Health and Environmental Sciences, University of L'Aquila, L'Aquila, Italy
[c] Department of Biotechnological and Applied Clinical Sciences, University of L'Aquila, L'Aquila, Italy
[d] Institute of Histology and Embryology, School of Medicine, Catholic University of the Sacred Heart, Rome, Italy
[e] Bone Physiopathology Group, Multifactorial Disease and Complex Phenotype Research Area, Bambino Gesù Children's Hospital, Rome, Italy
[f] Department of Sense Organs, Sapienza University of Rome, Rome, Italy
[g] Radiation Oncology Unit, University Hospital of Siena, Siena, Italy
[h] Sbarro Health Research Organization, Temple University, Philadelphia, PA, United States
[i] Department of Radiation Oncology, University and Spedali Civili Hospital, Brescia, Italy
[j] Department of Molecular and Translational Medicine, Division of Biotechnology, University of Brescia, Brescia, Italy
[k] Department of Oral and Maxillo-Facial Sciences, Sapienza University of Rome, Rome, Italy

ARTICLE INFO

Keywords:
PXD-101
Belinostat
Rhabdomyosarcoma
Differentiation therapy
Radioresistance

ABSTRACT

This study describes the *in vitro* and *in vivo* activity of PXD-101 (Belinostat), a novel hydroxamic acid-type pan-HDACs inhibitor characterized by a larger safety and efficacy, on myogenic-derived PAX3/FOXO1 fusion protein positive (RH30) or negative (RD) expressing rhabdomyosarcoma (RMS) cell lines. PXD-101 at low doses efficiently inhibited HDACs activity and counteracted the transformed phenotype of RMS by inducing growth arrest and apoptosis, affecting cancer stem cells population and inducing differentiation in RD. Notably, PXD-101 induced oxidative stress promoting DNA damages and affected the ability of RMS to assemble mitotic spindle. PXD-101 radiosensitized by inducing G2 cell cycle growth arrest, enhancing the radiation's ability to induce ROS accumulation and compromising both the ability of RMS to detoxify from ROS and to repair DNA damage. PXD-101 transcriptionally and post-transcriptionally affected c-Myc expression, key master regulator of rhabdomyosarcomagenesis and RMS radioresistance. All *in vitro* data were corroborated by *in vivo* experiments showing the cytostatic effects of PXD-101 when used alone and at low dose and its ability to promote the RT-induced killing of RMS. Taken together, our data confirm that altered HDACs activity plays a key role in RMS genesis and suggest PXD-101 as a valid therapeutic strategy particularly in combination with RT.

1. Introduction

Rhabdomyosarcoma (RMS) is the most frequent soft tissue sarcoma observed in pediatric patients [1]. Standard multimodality treatment by surgery, radiotherapy (RT) and chemotherapy (CHT) is often effective for localized and locally-advanced tumors [2,3]. Notably, treatment failure frequently occurs and is more common in patients that not received or received delayed RT [2,3], indicating the key role of this treatment in treating RMS [2–4]. However, despite tremendous advances in RT techniques, allowing dose escalation to tumor tissues and sparing of organs at risk, cure rates remain suboptimal also in patients receiving RT. Thus, it needs a better understanding of the molecular

* Corresponding author. Department of Radiotherapy, Policlinico Umberto I, "Sapienza" University of Rome, Rome, Italy.
E-mail address: francesco.marampon@uniroma1.it (F. Marampon).
[1] Equal contribution.

https://doi.org/10.1016/j.canlet.2019.07.009
Received 13 May 2019; Received in revised form 8 July 2019; Accepted 13 July 2019

Abbreviations

ARMS	Alveolar rhabdomyosarcoma
Akt	Protein kinase B
Akt^{PO4}	phosphorylated Protein kinase B
CXCR-4	C-X-C chemokine receptor type 4
CHT	Chemotherapy
c-Myc	myelocytomatosis virus oncogene cellular homolog
DMEM	Dulbecco's modified Eagle's medium
DSBs	DNA double-strand break
ELISA	enzyme-linked immunosorbent assay
ERKs	extracellular signal-regulated kinases
$ERKs^{PO4}$	phosphorylated extracellular signal-regulated kinases
ERMS	Embryonal rhabdomyosarcoma
FNRMS	Fusion-negative-rhabdomyosarcoma, FNRMS
FPRMS	Fusion-positive-rhabdomyosarcoma
FOXO1	forkhead-box-protein-O1
GI_{50}	Dose of PXD-101 able to reduce, by 50%, cell viability
GAPDH	Glyceraldehyde 3-phosphate dehydrogenase
H2AX	H2A histone family member X
γH2AX	phosphorylated H2A histone family member X
HDACs	Histone deacetylases
HDACi	Histone deacetylases inhibitor
IR	Ionizing Radiation
IC_{50}	Dose of PXD-101 able to reduce, by 50%, the HDACs activation status
LD_{50}	Dose of PXD-101 able to induce, by 50%, cell death
MAD2	mitotic arrest deficient 2
MYOD	Myogenic Differentiation 1
MyHC	myosin heavy chain
MTT	3-(4,5-Dimethylthiazol-2-yl)-2,5-Diphenyltetrazolium Bromide assay
MDA	microtubule-destabilizing agents
Oct-3/4	octamer-binding transcription factor-3/4
PAX3/7	encoding-paired-box-protein-3 or -7
PI3K	phosphatidyl inositol-4,5-bisphosphate-3-kinase
RMS	rhabdomyosarcoma
RT	Radiotherapy
ROS	Reactive oxygen species
Ras	rat sarcoma
RT-PCR	reverse transcription polymerase chain reaction
RNA	ribonucleic acid RTKs Receptor tyrosine kinase
RT	Radiotherapy
RMS	rhabdomyosarcoma

mechanisms determining radioresistance and to identify new radiosensitizing strategies.

RMS are currently subdivided into fusion-positive (FPRMS) or fusion-negative (FNRMS) depending on a distinctive chromosomal translocation generating the fusion of paired-box-3 or -7 (PAX3 or -7) with forkhead-box-O1 (FOXO1) genes [1]. On histological analysis, FPRMS cells show a peculiar alveolar-like tissue organization that is a hallmark of the alveolar subtype (ARMS), the more aggressive RMS form. FNRMS cells instead show an embryonal histology (ERMS) resembling muscle cell progenitors attempting to differentiate [1]. Furthermore, in addition to the fusion signatures, RMS often present alterations in RAS–PI3K signaling axis due to aberrant receptor tyrosine kinase (RTKs) activity [5,6].

Alteration on epigenetic mechanisms driven by histone deacetylases (HDACs) enzymes is emerging as critical for RMS progression [7]. HDACs participate in chromatin remodeling and affect gene expression [8]. When aberrantly expressed and/or activated they significantly impact on tumor progression and therapy resistance [9], being therefore considered attractive candidate targets for anticancer drugs and therapies [10]. To date, several HDAC inhibitors (HDACi) have been tested *in vivo* and *in vitro* for exerting a marked anti-tumoral activity [10] including versus RMS [11,12]. In the context of multimodality therapy approach, combination regimen for sarcomas appear to be more promising than monotherapy when using HDACi [13]; however, no studies have been conducted to investigate whether preventive HDACs inhibition could increment the efficacy of RT in RMS.

RT induces lethal DNA double strand Breaks (DSBs) and it is generally estimated that approximately two-thirds of DSBs are caused by the production of reactive oxygen species (ROS), indirect damage that, unlike the direct type, persists from hours to days after radiation [14]. Unfortunately, cancer cells [15,16], including RMS [17–19], frequently over-express molecular mechanisms that by detoxifying from ROS accumulation and promoting DSBs repair, efficiently counteract the therapeutic action of RT.

This study describes the *in vitro* and *in vivo* activity of PXD-101 (Belinostat), a novel hydroxamic acid-type pan-HDACs inhibitor characterized by a larger safety and efficacy, on FPRMS (RH30) or FNRMS negative (RD) RMS cell lines. Treatment of RMS cell lines with PXD-101 significantly inhibited tumour cell growth, reduced the stem-like cell population and promoted myogenic differentiation of surviving FNRMS cells. Furthermore, PXD-101 was able to radiosensitize RMS cells by affecting the radiation-induced activation of the detoxifying-from-ROS and DNA-repair mechanisms. All *in vitro* data were corroborated by *in vivo* experiments showing the cytostatic effects of PXD-101 when used alone and at low dose and its ability to promote the RT-induced killing of RMS. Taken together, our data confirm that altered HDACs activity plays a key role in RMS genesis and suggest PXD-101 as a valid therapeutic strategy particularly in combination with RT.

2. Materials and methods

2.1. Cell lines and pharmacological treatment

The human RMS RD (ERMS) and RH30 (AMRS) cell lines were obtained by American Type Culture Collection (Manassas, VA) and maintained in high-glucose Dulbecco's modified Eagle's medium (DMEM) supplemented with 10% fetal bovine serum (FBS), 1% v/v L-glutamine, 100 μg/ml streptomycin and 100 U/ml penicillin and grown at 37 °C in a humidified atmosphere of 5% CO2. DNA profiling using the GenePrint 10 System (Promega Corporation, Madison, WI) was carried out to authenticate cell cultures, comparing the DNA profile of our cell cultures with those found in GenBank.

2.2. HDAC activity-, cell viability-, proliferation- and caspases-assay

HDACs activity was evaluated by a colorimetric HDAC activity assay kit (Enzo Life Sciences GmbH). Cellular viability was measured by 3-(4,5-Dimethylthiazol-2-yl)-2,5-Diphenyltetrazolium Bromide assay (MTT). Cell count was performed by the Countess II Automated Cell Counter (ThermoFisher Scientific, Waltham, MA) and cell death identified by the trypan-blue exclusion assay (Life Technologies, Grand Island, NY). Caspase-Glo®3, 8 and 9 assays from Promega were used to measures caspase activity. All assays were performed according to the manufacturer's instructions.

2.3. Cell cycle analysis, morphological and immunofluorescence assays

A DNAcon3 kit (Dako, Glostrup, Denmark) was used for DNA staining Analysis was performed with FACS calibur, and the cell-cycle distribution was analyzed using Mod-Fit software (Verity Software House, Topsham, ME, USA) [20]. Morphological assessment and immunofluorescence assays were performed as already described [17].

2.4. Western blot and real-time analysis

Western blot analyses were performed as already described [21] by using the following primary antibodies: $p21^{WAF1}$ (C-19), $p27^{KIP1}$ (F-8), $p57^{KIP1}$ (KP39), $p19^{Ink4d}$ (E-11), Cyclin A (BF683), Cyclin D1 (M-20), Cyclin B1 (H-20), myelocytomatosis virus oncogene cellular homolog (c-Myc) (9E10), N-Myc (B.8.4.B), MAD2 (17D10), integrin β1 (M-106), phosphorylated extracellular signal-regulated kinase 1/2 ($ERK1/2^{PO4}$) (E-4), extracellular signal-regulated kinase (ERK1/2) (C-14, positive also for ERK1), p38 (H-147), phosphorylated Protein kinase B (Akt^{PO4}) (Ser473), Protein kinase B (H-136), MYOGENIN (F5D), H2A histone family member X (H2AX) (C-20), octamer-binding transcription factor-3/4 (Oct-3/4) (C-10) and Glyceraldehyde 3-phosphate dehydrogenase (GAPDH) (6-C5) by Santa Cruz Biotechnology; Myogenic Differentiation 1, (MYOD) (MAB3878) and myosin heavy chain (MyHC) (05–716) by EMD Millipore Corporation (Billerica, MA); phosphor-p38 (Thr180/Tyr182)(9211) and phosphorylated H2A histone family member X (γH2AX) (Ser139) (2577) by Cell Signaling Technology (Danvers, MA). Appropriate horseradish peroxidase (HRP)-conjugated secondary antibodies (Santa Cruz Biotechnology) were used for 1 h at room temperature. mRNA extraction, Real-Time and data analysis were performed as already described [22].

2.5. Migration, invasion assays and ste-like cells isolation

Wound healing and invasion assays were performed as already described [23]. Sphere-forming cells were obtained as described [18]. Stem cell markers in rhabdomyosarcoma cells were evaluated by staining with monoclonal antibodies conjugated with anti–CD13 and anti-C-X-C-chemokine receptor type 4 (CXCR4) (all from BD Biosciences, Buccinasco, Italy). Appropriate isotype controls for non-specific binding were used for each antibody. A minimum of 50,000 events were acquired for each sample by a flow cytometer (FACSCalibur, BD Biosciences) using CellQuest software (BD Biosciences) for data acquisition and analysis [18].

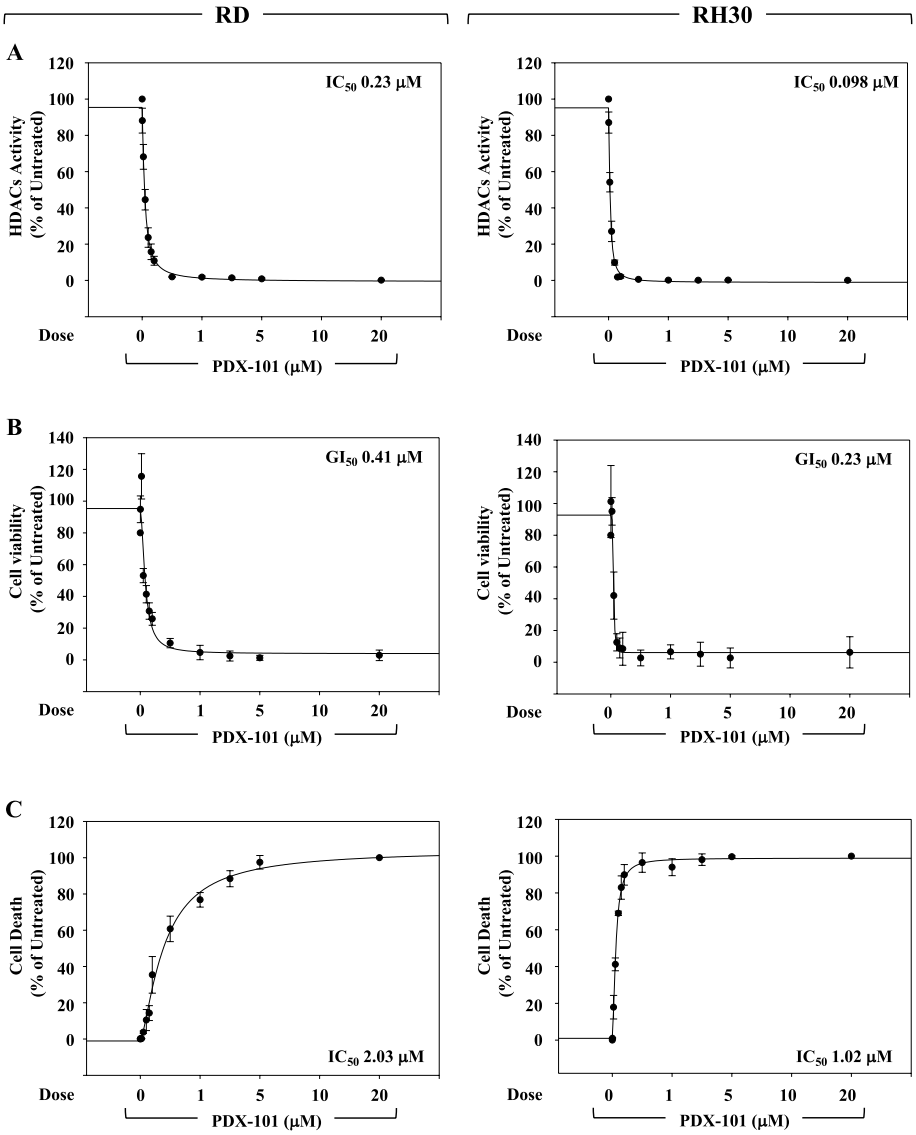

Fig. 1. PXD-101 efficiently affects HDACs activity and cell viability inducing cell death in a dose dependent manner in FNRMS and FPRMS rhabdomyosarcoma cells. Dose of PXD-101 able to reduce, by 50%, the HDACs activation status (Fig. A, IC_{50}), cell viability (Fig. B, GI_{50}) and to induce by 50%, the cell death, (Fig. C, LD_{50}) of RD and RH30 cell lines treated for 24 h with increasing doses of PXD-101 (0, 1, 5, 10, and 20 μM). Results represent the mean values of three independent experiments ± SD. Statistical significance: $^{*}p \leq 0.05$, $^{**}p \leq 0.01$, $^{***}p \leq 0.05$ compared with the respective control (Untreated cells).

2.6. In vitro radiation exposure and mitochondrial superoxide anion ($\cdot O2^-$) production assessment

Radiation was delivered at room temperature using an x-6 MV photon linear accelerator, as previously described [18]. Mitochondrial superoxide anion ($\cdot O2^-$) production assessment was performed by using MitoSOX Red (Thermo Fisher Scientific, Milan, Italy) as already described [17].

2.7. Animal research ethics statement, in vivo xenograft experiments and statistical analysis

This study was carried out in strict accordance with the recommendations of the European Community (EC) guidelines (2010/63/UE and DL 26/2014 for the use of laboratory animals) and in line with University guidelines (University of L'Aquila, Medical School and Science and Technology School Board Regulations, on the use of laboratory animals). Six-week-old female CD1 nu/nu mice were purchased from Charles River Laboratories Italia, SRL (Calco, Italy). All mice received subcutaneous flank injections of 1×10^6 RD or RH30 cells. Tumour growth was assessed as already described [21,23]. PXD-101 40 mg/kg was administered every day for twelve days starting the day before RT treatment. This protocol was chosen because a full inhibition of HDACs is guaranteed *in vivo* [23]. Mice were irradiated at room temperature using an Elekta 6-MV photon linear accelerator. Five fractions of 2 Gy were delivered every other day for a total dose of 12 Gy. A dose rate of 1.5 Gy/min was used with a source-to-surface distance (SSD) of 100 cm. Prior to irradiation mice were anesthetized and were protected from off-target radiation by a 3 mm lead shield. Before tumor inoculation mice were randomly assigned to 4 experimental groups. Each group was composed of 8 mice. One control group received intraperitoneal (i.p.) injection of 200 µl carrier solution; one group received i.p. injection of 40 mg/kg/dose of PXD-101 for 12 consecutive days; one group received RT (6 fractions of 2 Gy delivered 3

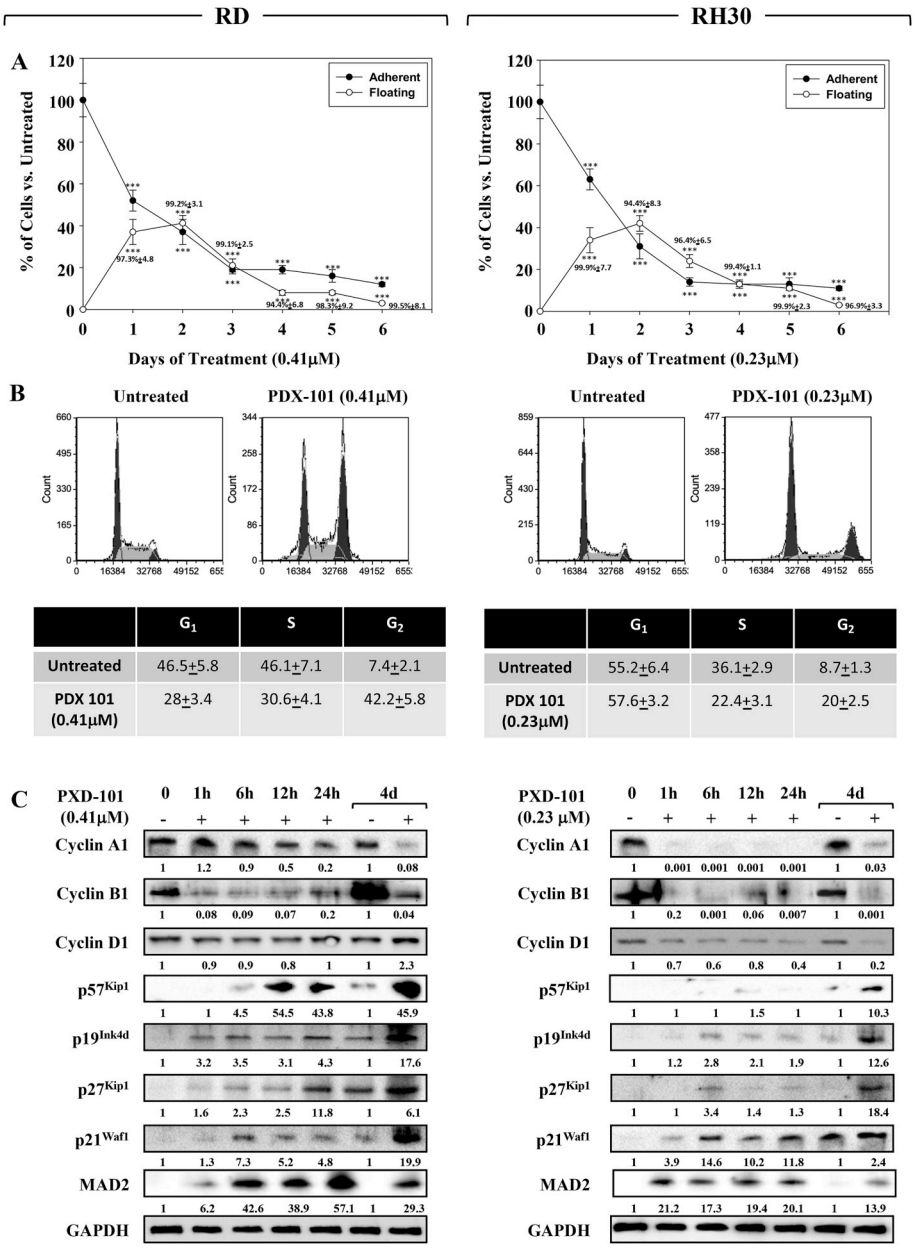

	G_1	S	G_2
Untreated	46.5±5.8	46.1±7.1	7.4±2.1
PDX 101 (0.41µM)	28±3.4	30.6±4.1	42.2±5.8

	G_1	S	G_2
Untreated	55.2±6.4	36.1±2.9	8.7±1.3
PDX 101 (0.23µM)	57.6±3.2	22.4±3.1	20±2.5

Fig. 2. PXD-101 concomitantly induces G_2 cells cycle arrest and death in FNRMS and FPRMS rhabdomyosarcoma cells. A. Effect of PXD-101 on cell number of adherent and floating RD (0.41 µM) and RH30 (0.23 µM) cells treated for increasing times (1,2,3,4,5 and 6 days). Cell viability on floating cells was measured by trypan blue dye exclusion test. Results represent the mean values of four independent experiments ± SD. Statistical significance: $^{*}p \leq 0.05$, $^{**}p \leq 0.01$, $^{***}p \leq 0.001$ compared with the respective control (Untreated cells). B. FACS analysis performed on RMS cells untreated (DMSO) or treated PXD-101 (RD 0.41 µM and RH30 0.23 µM) for 24 h. Representative of three different experiments (upper panel). Table showing the percentage of cell cycle phases in RD and RH30 cells ± PXD-101 (lower panel). Results represent the mean value of four independent experiments. C. Cell lysates from RD and RH30 cells ± PXD-101 (RD 0.41 µM and RH30 0.23 µM) at the indicated times were analysed by immunoblotting with specific antibodies for indicated proteins; GAPDH expression shows the loading of samples. Representative of two independent experiments.

times/week to a total dose of 12 Gy); one group received 40 mg/kg/dose of PXD-101 for 12 consecutive days, coupled with RT (6 fractions of 2 Gy delivered 3 times/week to a total dose of 12 Gy) delivered 24 h after the beginning of treatment with PXD-101 (Fig. 4). Experiments were stopped 12 days after the last treatment, animals sacrificed via carbon dioxide inhalation, and tumours removed and analysed. To compare different treatments, we considered as previously described [23]: (1) tumour volume, measured at different times; (2) tumour weight, measured at the end of experiment; (3) tumour progression (TP), defined as an increase > 50% of tumour volume with respect to baseline. Statistical analysis was performed as already described [21,23].

2.8. Key Resource Table

Resource	Source	Identifier
Antibodies		
anti-C-X-C- chemokine receptor type 4 (CXCR4)		
c-Myc	N/A	N/A
N-Myc		
p21 WAF1		
Antibodies		
anti-C-X-C- chemokine receptor type 4 (CXCR4)		
c-Myc	N/A	N/A
N-Myc		
p21 WAF1		
CellLine		
RD		
RH30		
Chemical		
2,5- Diphenyltetrazolium Bromide		
5-Dimethylthiazol-2-yl		
carbon dioxide		
DMEM	N/A	N/A
L- glutamine		
penicillin		
PXD-101		
streptomycin		
ProteinPeptide		
Akt	N/A	N/A
caspase		
ERKs	N/A	N/A
HDAC		

3. Results

3.1. PXD-101 inhibits HDACs inducing growth arrest and apoptosis of rhabdomyosarcoma cells

PXD-101 caused 50% of maximal inhibition of HDACs activity (IC_{50}) at 0.23 ± 0.05 μM in RD and 0.098 ± 0.01 μM in RH30 (Fig. 1A). The concentration able to affect 50% of maximal cell viability (GI_{50}) was 0.41 ± 0.06 μM in RD and 0.23 ± 0.02 μM in RH30 (Fig. 1B) whilst able to induce 50% of cell death (LD_{50}) was 2.03 ± 0.4 μM in RD and 1.02 ± 0.2 μM in RH30 (Fig. 1C). At GI_{50} concentration, PXD-101 induced growth arrest by 83.2 ± 7.2% in RD and 78.7 ± 8.3% in RH30 (Fig. 2A) and significantly increased the percentage of floating cells, resulting in the death of almost all cells (Fig. 2A, Percentage related to Floating Plot). Treating RMS with PXD-101 (GI_{50}) for 24 h increased the percentage of RMS in the G_2 phase of the cell cycle (Fig. 2B). According to G_2/M cell cycle arrest, PXD-101 down-regulated the expression of the cell cycle promoters Cyclin A and Cyclin B1 in both RMS cell lines and of Cyclin D1 only in RH30 (Fig. 2C) whilst up-regulated the expression of cell cycle inhibitors $p57^{KIP1}$, $p19^{Ink4d}$, $p21^{WAF1}$and $p27^{KIP1}$ in both RMS cell lines (Fig. 2C). Furthermore, PXD-101 up-regulated the expression of MAD2 (Fig. 2B), bio-marker of mitotic defects on spindle assembly checkpoint [24]. Notably, 24 h later, the percentage of apoptotic cells resulted increased by PXD-101 (GI_{50}) of 21.3 ± 3.5% in RD and 37.2 ± 6.1% in RH30 (Fig. 3A) as well as the activation of caspase-9 and -3. (Fig. 3B). Treatment did not increase the activation of caspase 8 as well as the cleavage/activation of PARP (Fig. 3B).

3.2. PXD-101 counteracts in vitro migration/invasion, affects self-renewal ability and leads to differentiation of rhabdomyosarcoma cells

Wound healing assays, in which the same fields of confluent cells were pictured immediately after the scratch (time 0 h) and again after 24 h of PXD-101 (GI_{50}) incubation, shows that drug treatment decreased the level of wound closure to 71.3 ± 8.5% in RD (Fig. 4A, Left Panel) and 49.2 ± 9.1% in RH30 (Fig. 4A, Right Panel). The matrigel invasion assay shows that PXD-101 (GI_{50}) reduced invasive abilities by 93.2 ± 1.2% in RD (Fig. 4B, Left Panel) and 88.8 ± 4.3% in RH30 (Fig. 4B, Right Panel) compared to untreated. Immunoblotting analysis shows that PXD-101 down-regulated the expression of c-Myb, β-catenin and Integrin-β1 (Fig. 4C), key regulators of metastatic potential of RMS cells [25–27]. 6 days of PXD-101 treatment (GI_{50}) induced substantial

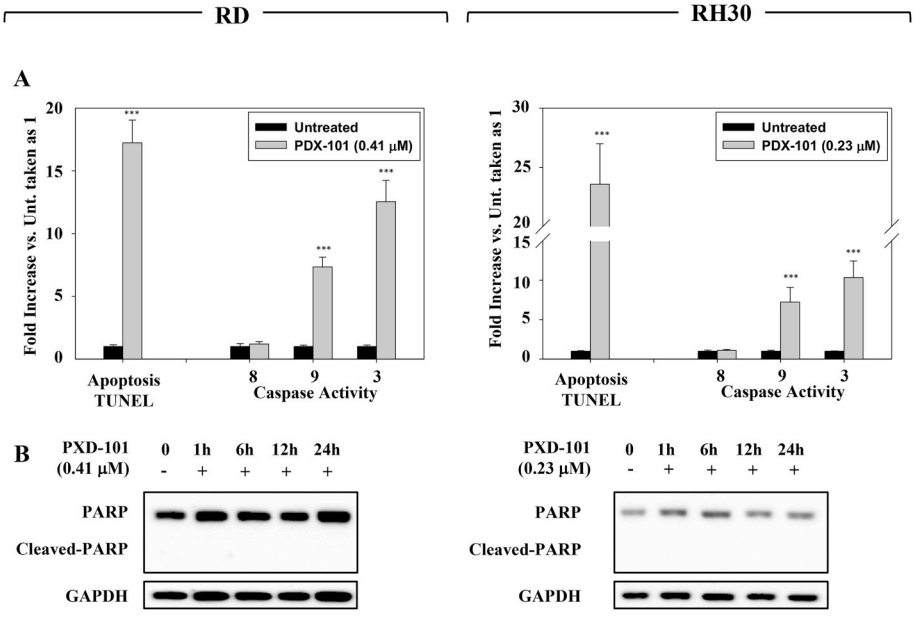

Fig. 3. PXD-101 induces caspase 9/3-mediated intrinsic caspase pathway activation without affecting the cleavage/activation of PARP in FNRMS and FPRMS rhabdomyosarcoma cells. A. Fold increase of apoptotic cells assessed by TUNEL (Apoptosis TUNEL bars) and activation levels of caspase-8, caspase-9 and caspase-3 (Caspase activity bars) measured by human caspase ELISA assay 24 h after treating with PXD-101 RD (0.41 μM) and RH30 (0.23 μM) cells. Results represent the mean values of four independent experiments ± SD. Statistical significance: $^{*}p \le 0.05$, $^{**}p \le 0.01$, $^{***}p \le 0.001$ compared with the respective control (Untreated cells). B. Cell lysates from RD and RH30 cells ± PXD-101 (RD 0.41 μM and RH30 0.23 μM) at the indicated times were analysed by immunoblotting for the expression levels of uncleaved (PARP) and the cleaved form (Cleaved-PARP) of PARP; GAPDH expression shows the loading of samples. Representative of two independent experiments.

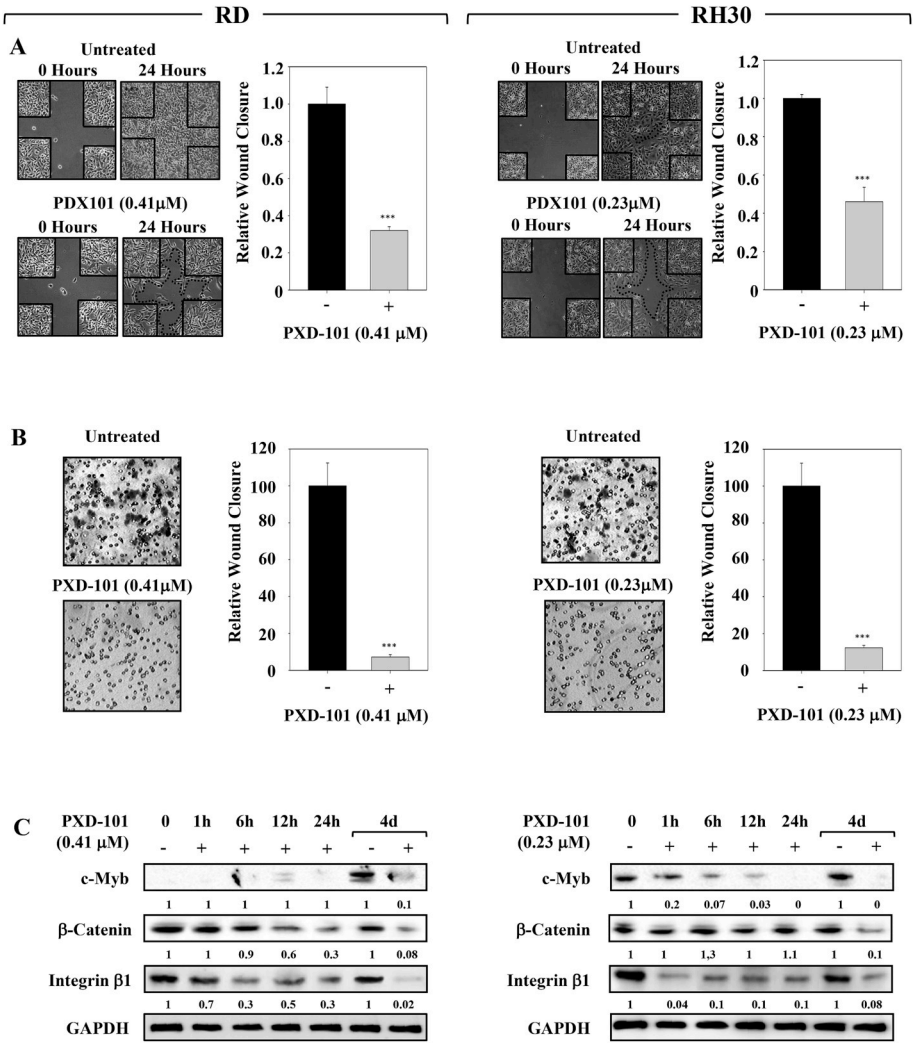

Fig. 4. PXD-101 decreases wound closure and invasion ability affecting the expression related-biomarkers in FNRMS and FPRMS rhabdomyosarcoma cells. A. Wound healing experiments in RD and RH30 cells. A scratch was made at time 0 and maintained or not for 24 h in the presence of PXD-101. The dotted lines represent the edges of the wound. Photographs were taken under light microscope (10x magnification). The migration index was plotted in bar graphs. B. Matrigel invasion assay for RD and RH30 cells treated with 0.41 μM or 0.23 μM, respectively were allowed to invade for 24 h in serum-free medium. Pictures shown are the most representative from three independent experiments. The graph represents absorbance at 595 nm after incubation of the membranes with deoxycholic acid. Results represent the mean values of four independent experiments ± SD. Statistical significance: $^{*}p \leq 0.05$, $^{**}p \leq 0.01$, $^{***}p \leq 0.001$ compared with the respective control (Untreated cells). C. Cell lysates from RD and RH30 cells ± PXD-101 (RD 0.41 μM and RH30 0.23 μM) at the indicated times were analysed by immunoblotting with specific antibodies for indicated proteins; GAPDH expression shows the loading of samples. Representative of three independent experiments.

change in morphology, with more elongated cellular bodies in RD and a spindle shape in RH30 (Fig. 5A), suggestive of the acquisition of a myogenic-like phenotype. Immunoblotting analysis shows that PXD-101 (GI_{50}) differently induced the expression of myogenic markers MYOD, MYOGENIN and MyHC in RMS cell lines (Fig. 5B). In RD cells, the transient (6 h) up-regulation of MYOD was followed by the persistent up-regulation of MYOGENIN (24 h–4 days) and finally by the expression Myosin (Figs. 5B and 4 days). In RH30 cells we noticed only a transient up-regulation of MYOGENIN (Fig. 5B). PXD-101 (GI_{50}) in stem cell medium reduced the formation of cancer stem-like cells enriched in rhabdospheres by 84.1 ± 3.1% in RD and 92.5 ± 1.2% in RH30 (Fig. 5C), reduced the number of CD133 (Fig. 5D and 69.5 ± 5.4% in RD and 87.6 ± 4.7% in RH30) and CXCR4 (Fig. 5D and 73.3 ± 5.4% in RD and 92.8 ± 4.7% in RH30) positive cells and the protein expression of Oct-3/4 and nanog (Fig. 5E) induced by stem cell medium.

3.3. PXD-101 affects the constitutive activation of MEKs/ERKs and PI3K/Akt signal transduction pathways and down-regulated the pathological accumulation of c-myc

The aberrant activation of MAPK and PI3K/Akt signal transduction pathways [5,6,28,29] and expression of related downstream targets including c-Myc promote and sustain the transformed phenotype of RMS cells [5,6,28–31]. PXD-101 (GI_{50}) stably and persistently inhibited ERKs both in RD and RH30 cells (Fig. 6A). p38 resulted phosphorylated/activated in RD from 6 to 24 h of treatment and just after 1 h of treatment RH30 cell lines (Fig. 6A). Akt was efficiently and persistently inhibited in RD but not in RH30 cells (Fig. 6A). Immunoblotting shows that PXD-101 rapidly (1 h) and persistently (4 days) down-regulated the expression of c-Myc protein both in RD and RH30 (Fig. 6B). No modulation were described on N-Myc protein expression levels (Fig. 6B), known to be amplified in ARMS but not in ERMS [32]. RT-PCR shows that PXD-101down-regulated c-Myc mRNA levels starting from 12 h in RD and 1 h in RH30 (Fig. 6C).

3.4. PXD-101 radiosensitizes by improving the ability of the RT to induce ROS-mediated DSBs

PXD-101 (GI_{50}) pre-treatment significantly reduced the ability of RMS to form colonies after 4 Gy of irradiation (Fig. 7A) without affecting the increase on phosphorylation/activation levels of H2AX (γ-H2AX), bio-marker of DNA double strand break damages [33], induced by RT (Figs. 7B and 3 hours, PXD-101 + RT *vs.* RT). However, 24 h after RT, PXD-101 pre-treatment counteracted the ability of RMS to restore γ-H2AX to basal levels (Fig. 7B and 24 h, PXD-101 + RT *vs.* RT). Notably, PXD-101 *di per se* induced a rapid (3 h) and persistent (24 h) accumulation of γ-H2AX (Fig. 7B, PXD-101 *vs.* Untreated). Roughly two-thirds of radiation-mediated DNA damage is caused by indirect effects from ROS [16] which production has been shown to be efficiently restrained by RMS [17]. Assessing the effects of HDAs inhibition on RT-induced oxidative stress, we found that the mitochondrial-derived ROS production induced by RT was rapidly (5 min) and

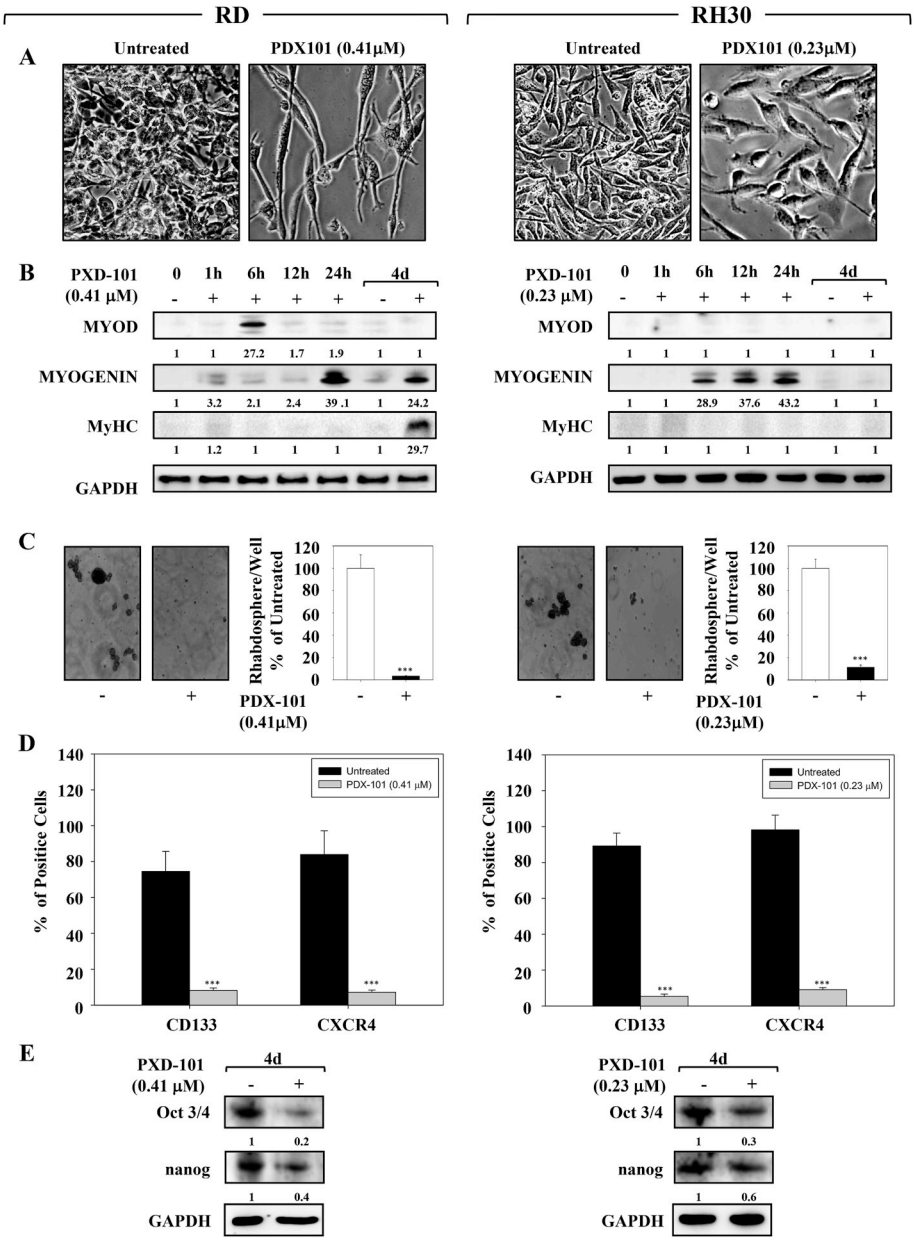

Fig. 5. PXD-101 counteracts the stem-like phenotype and triggers morphology changes in both RMS and myogenic differentiation in FNRMS. A. Cellular morphology of RMS cells untreated or treated with PXD-101 (RD 0.41 μM and RH30 0.23 μM) for 6 days was analyzed under light microscope at X20 magnification. Representative of three independent experiments. B. Cell lysates from RD and RH30 cells untreated (−) or treated (+) with PXD-101 (RD 0.41 μM and RH30 0.23 μM) for indicated times were analysed by immunoblotting with specific antibodies for indicated proteins; GAPDH expression shows the loading of samples. Representative of two independent experiments. C. Representative microphotographs of RD and RH30 cells in stem cell medium after 15 days of incubation in the absence (−) or in the presence of PXD-101 (RD 0.41 μM and RH30 0.23 μM). D Histograms of percentage of CD133 or CXCR4 positive cells determined by FACS analysis. Results represent the mean values of four independent experiments ± SD. Statistical significance: $^{*}p \leq 0.05$, $^{**}p \leq 0.01$, $^{***}p \leq 0.001$ compared with the respective control (Untreated cells). E. Cell lysates from tumorsphere from RD and RH30 cells untreated (−) or treated (+) with PXD-101 (RD 0.41 μM and RH30 0.23 μM) were analyzed by immunoblotting with specific antibodies for indicated proteins; GAPDH expression shows the loading of samples. Representative of two independent experiments.

persistently (12 h) improved by PXD-101 (GI_{50}) (Fig. 7C, PXD-101 + RT *vs.* RT), and that PXD-101 efficiently counteracted the ability of RMS to restore to basal levels ROS production (Fig. 7C and 12 h, RT *vs.* PXD-101 + RT). Notably, PXD-101 *di per se* rapidly and persistently increased ROS production (Fig. 7B, Untreated *vs.* PXD-101).

3.5. PXD-101 counteracts the RT-mediated activation of sensors, transducers and effectors proteins involved in the regulation of cell cycle checkpoints and involved in DSBs repair

Upon DNA damage, cells stop proliferation at cell cycle checkpoints, which provides them time for DSBs repair [34]. As shown in Fig. 8A, PXD-101 (GI_{50}) efficiently inhibited the RT-induced rapid and transient (3 h) phosphorylation/activation of Chk1 and ChK2 (Fig. 8A), known to result in the activation of the cell cycle checkpoints [35]. PXD-101 pre-treatment counteracted RT-induced phosphorylation/activation of DNA-PKCs and Brca1 and expression of Ku70 and Rad51 (Fig. 8A, RT *vs.* PXD-101 + RT). Notably, PXD-101 *di per se* induced phosphorylation/activation of DNA-PKCs however at significantly lower levels than those reached after RT (Fig. 8A, RT *vs.* Untreated). In both cell lines, PXD-101 efficiently restrained the phosphorylation/activation of ERKs, known to sustain RMS radioresistance [18,19].

3.6. PXD-101 inhibits tumour growth and radiosensitizes RMS in in vivo xenograft mouse models

For *in vivo* experiments, when tumour volume reached 85–100 mm^3 (T0), PXD-101 (40 mg/kg) [23] or vehicle (PBS) was administered for 12 consecutive days by intraperitoneal injection. RT treatment (2 Gy) was performed every other day, for 6 applications. Tumour volumes were measured every 4 days for a period of 24 days after the start of treatment in untreated (vehicle), PXD-101-treated (PXD-101), irradiated (RT) and PXD-101/irradiated (PXD-101 + RT) tumours (Fig. 9A). The rate of tumour growth was found to be markedly reduced by PXD-101 treatment, with a 45.7% and 47.6% reduction in tumour growth being observed at the end of treatment in RD and RH30 xenografted mice, respectively (Fig. 9A, PXD-101 *vs.* Untreated). RT slightly affected the growth of tumours in RD whilst no effects were described

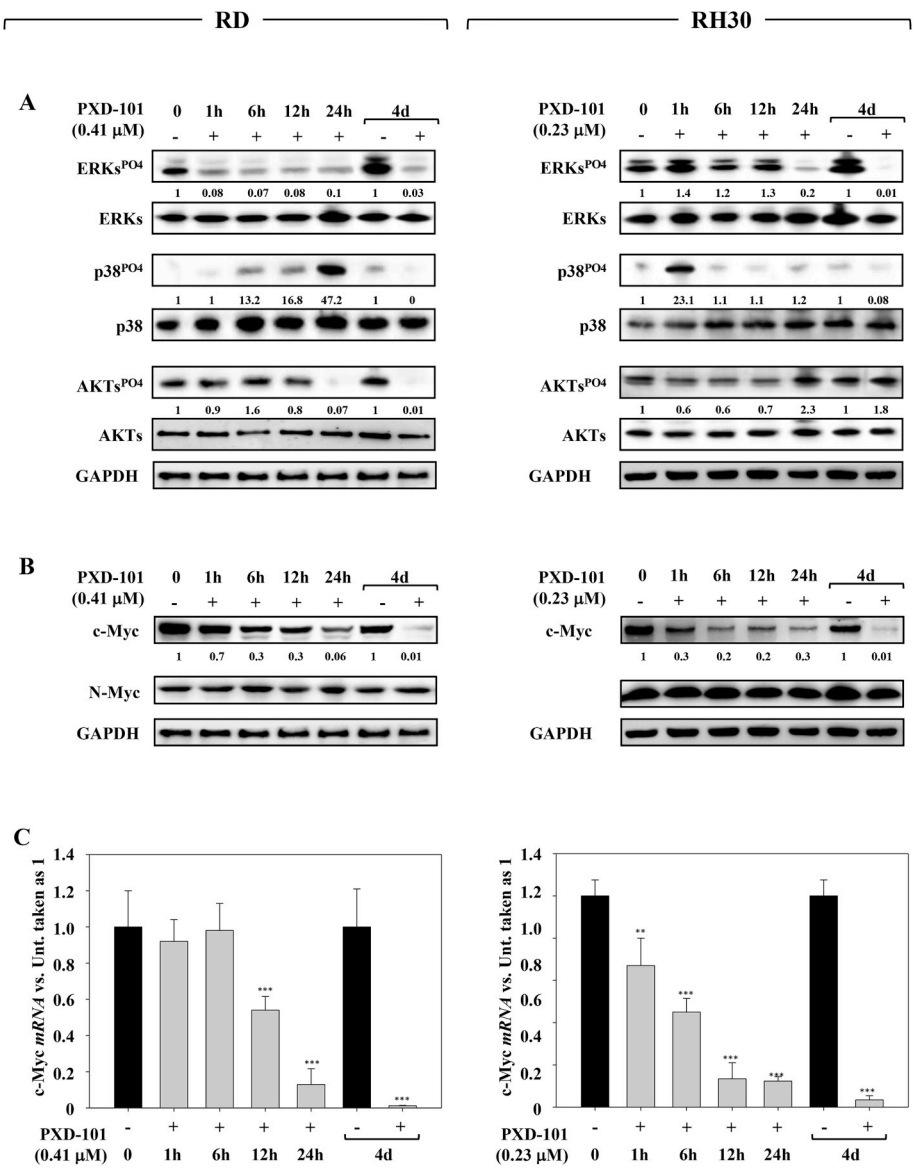

Fig. 6. PXD-101 inhibits rhabdomyosarcoma-related pro-oncogenic signal down-regulating the expression of c-Myc . A and B. Cell lysates from RD and RH30 cells untreated (−) or treated (+) with PXD-101 (RD 0.41 μM and RH30 0.23 μM) for indicated times were analysed by immunoblotting with specific antibodies for indicated proteins; GAPDH expression shows the loading of samples. Representative of two independent experiments. B. RT-PCR was performed to investigate the expression levels of c-Myc mRNA. Results represent the mean values of four independent experiments ± SD. Statistical significance: $^{*}p \leq 0.05, ^{**}p \leq 0.01, ^{***}p \leq 0.001$ compared with the respective control (Untreated cells). C. Gene expression of c-Myc was investigated by real-time PCR, at indicated times. The gene expression was referenced to the ratio of the value of interest and basal conditions. The value of basal conditions was reported equal to 1. Single results are representative of three different experiments performed in triplicate. Statisticalanalyses: *p < 0.05, **p < 0.01, ***p < 0.001 vs. Untreated.

in RH30 xenografted mice (Fig. 9A, RT *vs.* Untreated). Notably, in mice treated with PXD-101 + RT, at the end of the experiment, tumor volumes were lower than those measured at the beginning of treatment, respectively by 49.3% in RD and 60.9% in RH30 (Fig. 9A, PXD-101 + RT, 24th day *vs.* 0 day). Tumour weights in mice treated with PXD-101 decreased significantly ranging from 40 to 60% in RD and 30–50% in RH30 PXD-101 and from 70 to 90% in RD and 80–90% in RH30 in PXD-101 + RT treated mice, in comparison to controls (Fig. 9B). The number of mice with tumour progression (TP) significantly differed across the groups (Fig. 9C). In the vehicle group, tumour progression occurred both in RD and RH30 xenografted mice within 4 days after the beginning of treatment (Fig. 9C, Untreated). In the RT group, tumour progression occurred within 4 days in RH30 and 8 days in RD after the beginning of irradiation treatment (Fig. 9C, RT). The treatment with PXD-101 significantly improved the TP compared to vehicle or RT (Fig. 9C, PXD-101). In the PXD-101 group, tumour progression occurred from the 16th day in RD and 8th in RH30 after the beginning of treatment and never completed (Fig. 9C, PXD-101). The most evident improvement was documented when PXD-101 was coupled with RT: in this group, no tumour progression occurred both in RD and RH30 (Fig. 9C, PXD-101 + RT).

4. Discussion

In the present study we have demonstrated for the first time the effectiveness of a pan-HDAC inhibitor called PXD-101 (Belinostat) on RMS, a highly malignant myogenic tumor that mainly affects children [1]. As detected through *in vitro* and *in vivo* experiments, PXD-101 treatment counteracted tumor growth by cell cycle arrest and cell apoptosis/necrosis. Importantly, the broad impact of PXD-101 on both FPRMS and FNRMS tumors is relevant in the clinical setting, since detection of the PAX3-FOXO1 signature represents a critical parameter for assessing risk stratification and treatment allocation in RMS patients [1].

Low doses of PXD-101 were sufficient to inhibit HDACs activity and promote G2\M cell growth arrest in RMS cells, as evidenced by deregulation of Cyclin B1 and $p21^{Waf1}$, two master regulators of the cell cycle involved in the transition from G2 to M phase [36]. Furthermore, PXD-101 treatment led to an increased expression of MAD2, a key component of the mitotic checkpoint configuring as a “waiting signal” that has been shown to be activated in the presence of DSBs [24] or when the microtubules are not correctly attached to the kinetochore [37]. MAD2 is considered one of the most important tumor suppressor genes since its depletion correlates with tumor onset and progression

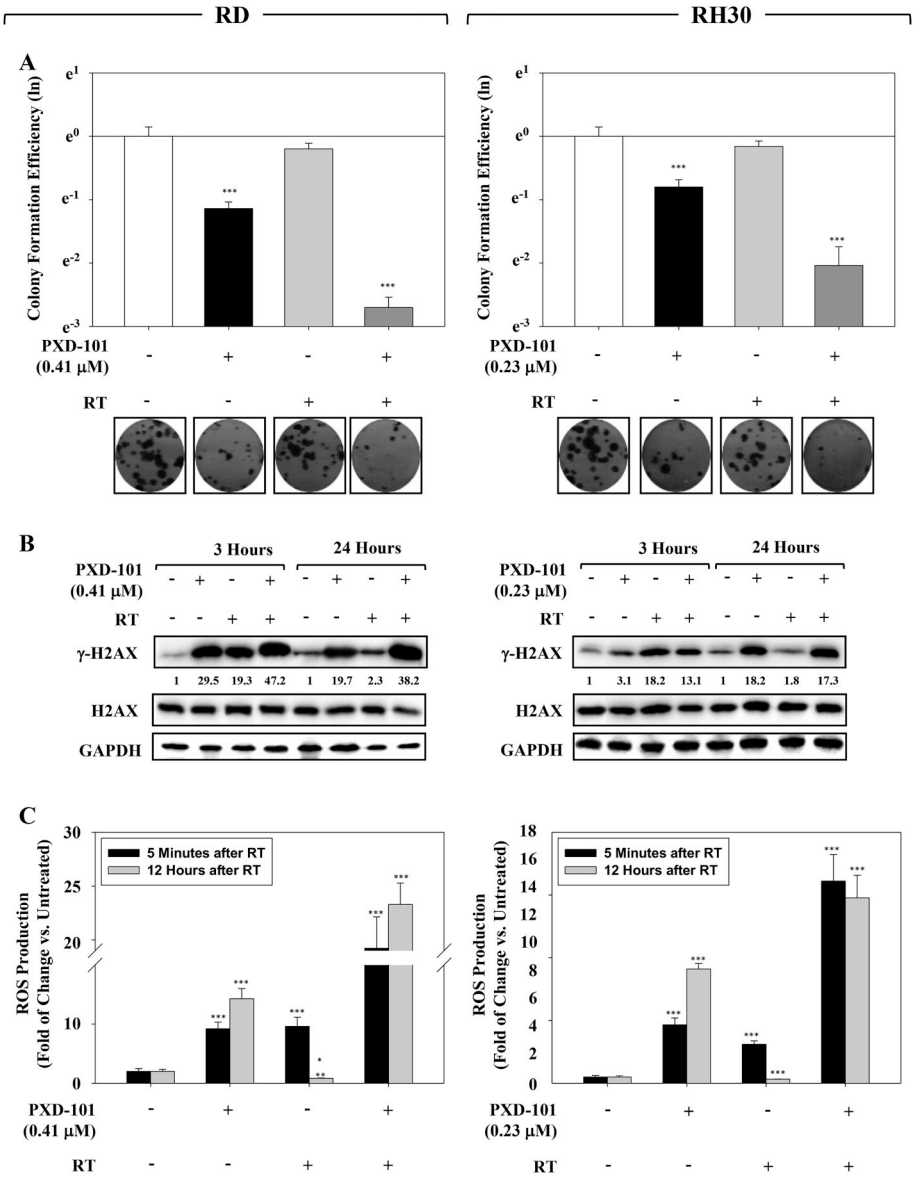

Fig. 7. PXD-101 *in vitro* radiosensitizes FNRMS and FPRMS rhabdomyosarcoma cells. A. Clonogenic assay of the RMS lines with (+) or without (−) PXD-101 (RD 0.41 μM and RH30 0.23 μM) and 4 Gy of irradiation treatments. Crystal violet stained cultures 14 days after PXD-101, RT, or combined treatment. B) Cell lysates from tumoursphere from RD and RH30 cells untreated (−) or treated (+) with PXD-101 (RD 0.41 μM and RH30 0.23 μM) were analyzed by immunoblotting with specific antibodies for indicated proteins; GAPDH expression shows the loading of samples. Representative of two independent experiments. C) Mitochondrial superoxide anion production was assessed by MitoSox Red staining, 5 min or 12 h after RT in untreated (−) or treated (+) with PXD-101 RMS cells (RD 0.41 μM and RH30 0.23 μM). Data were expressed as fold of change vs. untreated cells. Results represent the mean values of four independent experiments ± SD. Statistical significance: $^{*}p \le 0.05$, $^{**}p \le 0.01$, $^{***}p \le 0.001$ compared with the respective untreated cells.

[38]. It has been shown that restoring MAD2 expression can overwhelm the resistance of cancer cells to several microtubule-destabilizing agents (MDA) [39]. In light of this, since MDA treatment has been shown to be not very effective in RMS [40], a combined strategy together with PXD-101 could improve the therapeutic response in a MAD2-dependent fashion.

We also found PXD-101 to act as a trigger of cell death by activation of the intrinsic caspase9/caspase3 pathway in a PARP-independent manner [41]. Whereas both caspase activation and PARP cleavage are hallmarks of apoptosis [41], the failure in PARP cleavage by caspases has been shown to promote the induction of necrosis during apoptosis, especially in response to excessive ROS accumulation [42]. Hence, these data suggest that PXD-101 would act as a pro-apoptotic and –necrotic factor by inducing ROS elevation. In addition, we found the effects of PXD-101 slightly differing depending on the cell lines analyzed, since the alveolar RH30 cells carrying the PAX3-7/FOXO1 fusion gene underwent apoptosis rather than necrosis in response to the HDACs inhibitor.

In normal skeletal muscle, HDACs activity has been shown to impair the myogenesis process [43]. Likewise, HDACs inhibition by PXD-101 treatment promoted clearly visible changes in RD cell morphology, which was characterized by cell elongation that was consistent with the expression of myogenic markers predicting differentiation like MYOD, MYOGENIN and MyHC. In contrast, PXD-101 treatment failed to induce such effects in RH30 cells, which are known to be very refractory to differentiation stimuli.

In RD cells, the pro-differentiating effects of PXD-101 required the inactivation of MEKs/ERKs/c-Myc signaling axis [17,18,27,30,44], the up-regulation of $p57^{KIP1}$, $p27^{KIP1}$ and $p21^{Waf1}$ [45,46] and p38 activation [47], which are all critical events to force myogenesis in normal and malignant myogenic progenitors. In particular, we found PXD-101 inhibiting the RAS/MEKs/ERKs signaling, leading to a downstream deregulation of c-Myc expression both at transcriptional and post-transcriptional levels. These results are in line with our previous findings showing that the RAS/MEKs/ERKs signaling axis plays a pivotal role in RMS cell proliferation, enrichment of cancer stem cells (CSCs) and radioresistance through abnormal stabilization and accumulation of c-Myc [17,27,30]. Still, the mechanisms by which PXD-101 interferes with the RAS/MEKs/ERKs signaling to activate the myogenesis process require further investigation.

We further validated the efficacy of PXD-101 in reducing the expression of CD133, CXCR4, nanog and oct-3/4 markers, which predict a reduced number of CSCs, the main drivers of cancer onset, progression, metastasis and therapy resistance [48]. CSCs reside in an

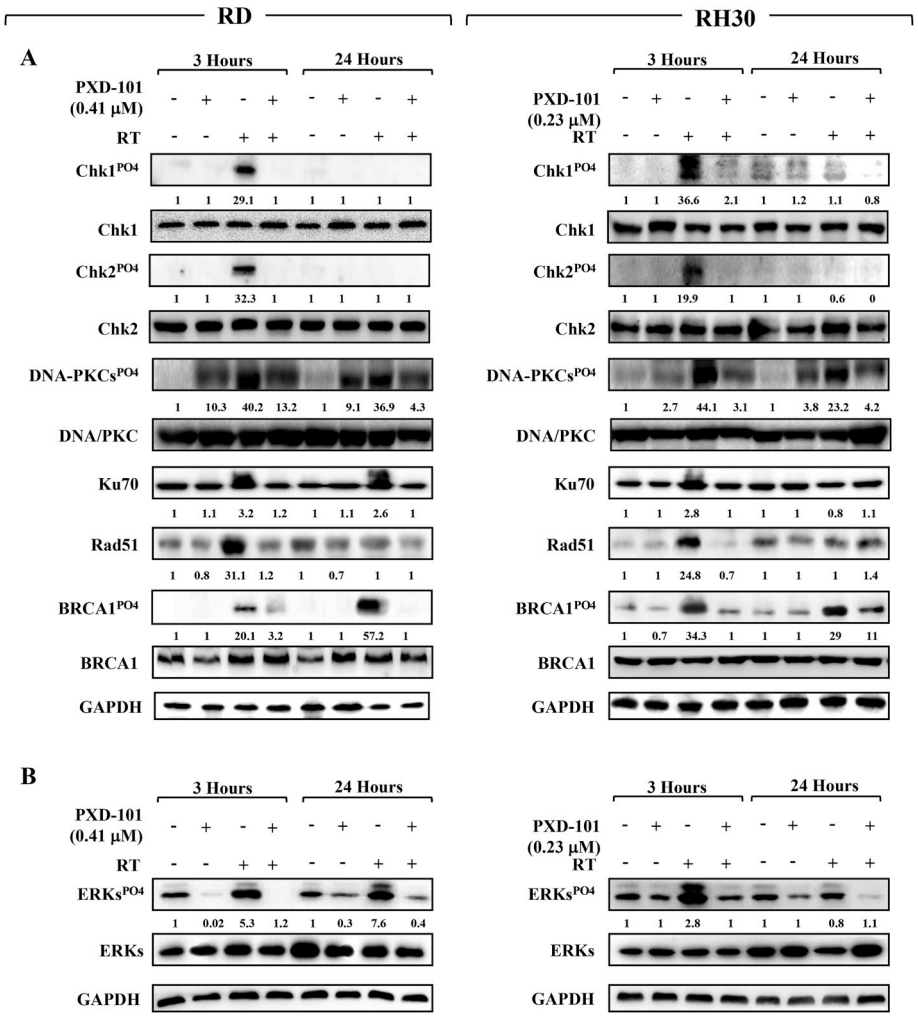

Fig. 8. PXD-101 affects the molecular mechanism controlling RMS responsiveness to RT and RT-induced ERKs activation. A and B. Cell lysates from RD and RH30 cells untreated (−) or treated (+) with PXD-101 (RD 0.41 μM and RH30 0.23 μM) and 4 Gy of irradiation treatments, collected 3 and 24 h after RT, were analyzed by immunoblotting with specific antibodies for indicated proteins; GAPDH expression shows the loading of samples. Representative of two independent experiments.

undifferentiated cell state and have the ability to regenerate intratumor heterogeneity after chemotherapy and radiotherapy, giving rise to recurrence. Such reduction in stemness markers induced by PXD-101 was indeed corroborated by a significant reduction of cell migration/invasion *in vitro*. Hence, the multiple ability of PDX-101 to induce differentiation and counteract cancer stemness is of considerable importance to halt tumor aggressiveness. The so called “differentiation therapy” has already been successfully tested in patients with acute promyelocytic leukemia [49] and is considered a valid approach for solid tumors, including sarcomas [50].

Our data pointed out the efficacy of PDX-101 as radiosensitizer for RMS treatment because of its ability of raising the intracellular ROS levels causative of DNA damage, even impairing the non-homologous end joining (NHEJ) and homologous recombination (HR) pathways involved in DNA repair. The combination of PDX-101 pre-treatment followed by RT on xenografted tumors promoted an important reduction in tumor volume and weight compared to RT alone. In these conditions, we evidenced a critical property of PDX-101 in limiting the activity Chk1 and Chk2, key regulators of the cell cycle checkpoints that elicit a delay in the cell cycle progression to permit DNA repair [51]. A number of inhibitors targeting Chks activity has indeed been developed for therapeutic purposes [52], and our current data indicate that PXD-101 could work as a “pan-Chk inhibitor”, increasing consistently the RT effects and eventually triggering both apoptosis and mitotic catastrophe-mediated cell death [53], the later appearing to be dominant.

In conclusion, data collected here indicate PXD-101 as a valuable drug with a pro-differentiating/radiosensitizer role for testing novel combined therapeutic approaches.

Founding

This research did not receive any specific grant from funding agencies in the public, commercial, or not-for-profit sectors.

Declarations of interest

None.

Author contributions

FM, VDN, IP, and FP initiated the research, developed the concept of the paper, designed the study, and analyzed and interpreted the data; BMS, IF, SC and CC performed experiments; MT, FDF, DM SC, PT and MM performed experiments regarding irradiation *in vitro*; GLG, ADF and CF performed experiments regarding irradiation *in vivo*; AF, AP, RM and VT supervised and wrote the manuscript.

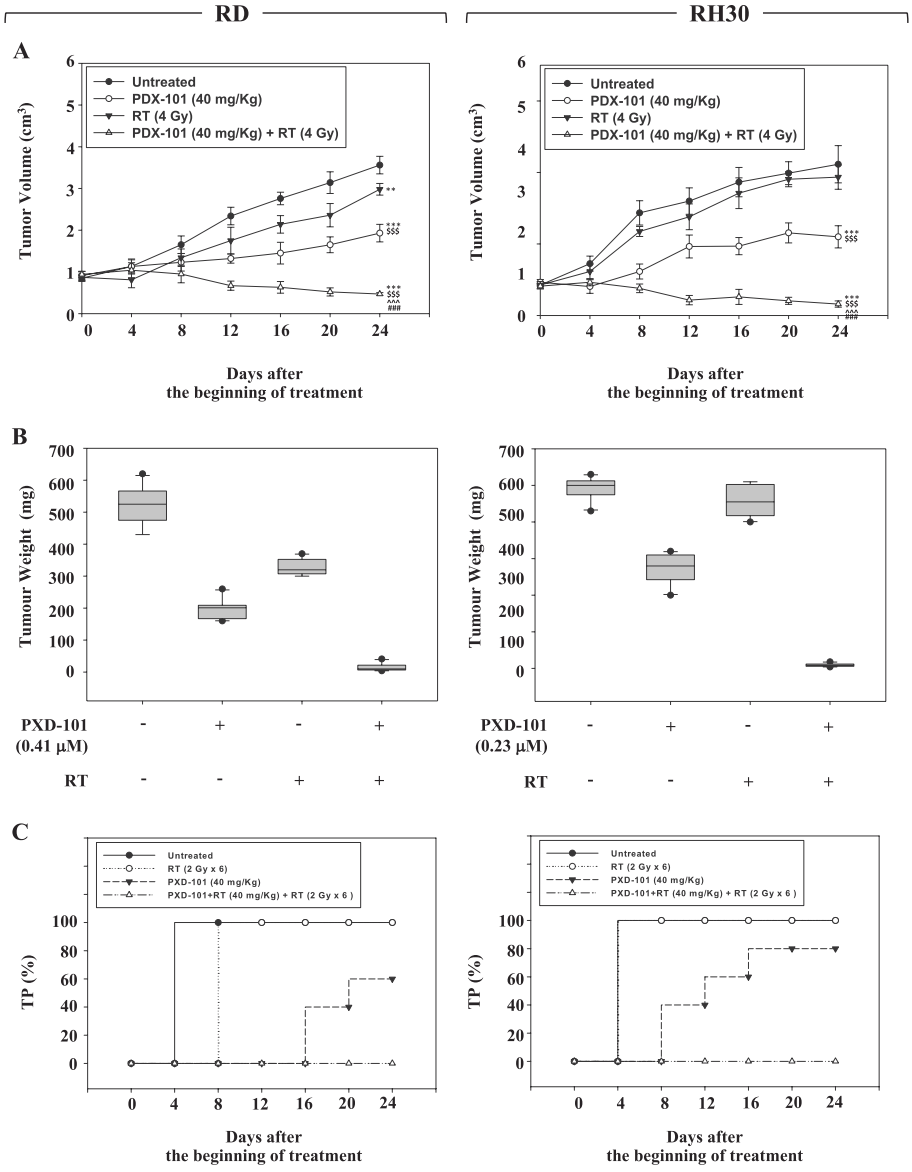

Fig. 9. Effects of PXD-101 combined or not with irradiation on *in vivo* tumour growth. A. Growth curve of tumour volumes from xenografted RD and RH30 cell lines, untreated (Untreated), PXD-101-treated (PXD-101), irradiated (RT), PXD-101-pretreated and irradiated (RT + PXD-101). Tumour volumes were evaluated as describes in methods and represent the mean ± SEM of 10 mice. The upper panel shows the sequential treatments of xenografted mice started when tumours reached a volume of approximate 85–100 mm^3. PXD-101 (40 mg/kg) was administered for 12 consecutive day and before each irradiation, administered on alternate days. Results represent the mean values ± SD. Statistical significance: $^{*}p \le 0.05$, $^{**}p \le 0.01$, $^{***}p \le 0.001$ compared with the respective untreated mice; $^{\$}p \le 0.05$, $^{\$\$}p \le 0.01$, $^{\$\$\$}p \le 0.001$ compared with the respective RT-treated mice; $^{\wedge}p \le 0.05$, $^{\wedge\wedge}p \le 0.01$, $^{\wedge\wedge\wedge}p \le 0.001$ compared with the respective PXD-101-treated mice; $^{\#}p \le 0.05$, $^{\#\#}p \le 0.01$, $^{\#\#\#}p \le 0.001$ compared with the respective PXD-101 + RT-treated mice. B. Tumour weights in mice untreated or treated with PXD-101, RT or combined treatment. C. Kaplan-Meier estimates for rates of progression for untreated, PXD-101, RT, or PXD-101 + RT combination in RMS-derived tumours.

Acknowledgements

We are grateful to “FIVA Confcommercio” and University of Rome, Sapienza for supporting our work, grant ID FIVAMARAM PONSAPIENZA. We are grateful to Dott. James Ashley from University of Manchester, UK, for the language editing.

References

[1] S.X. Skapek, A. Ferrari, A.A. Gupta, P.J. Lupo, E. Butler, J. Shipley, F.G. Barr, D.S. Hawkins, Rhabdomyosarcoma. Nat Rev Dis Primers. 5 (2019) 1.

[2] J.A. Bradley, M.L. Kayton, Y.Y. Chi, D.S. Hawkins, J. Tian, J. Breneman, S.L. Wolden, D. Walterhouse, D.A. Rodeberg, S.S. Donaldson, Treatment approach and outcomes in infants with localized rhabdomyosarcoma: a report from the soft tissue sarcoma committee of the children's oncology group, Int. J. Radiat. Oncol. Biol. Phys. 103 (2019) 19–27.

[3] E. Bompas, L. Campion, A. Italiano, A. Le Cesne, C. Chevreau, N. Isambert, M. Toulmonde, O. Mir, I. Ray-Coquard, S. Piperno-Neumann, E. Saada-Bouzid, M. Rios, J.E. Kurtz, C. Delcambre, P. Dubray-Longeras, F. Duffaud, M. Karanian, F. Le Loarer, P. Soulié, N. Penel, J.Y. Blay, Outcome of 449 adult patients with rhabdomyosarcoma: an observational ambispective nationwide study, Cancer Med 7 (8) (2018 Aug) 4023–4035, https://doi.org/10.1002/cam4.1374 Epub 2018 Jun 28.

[4] A. Kaushal, D. Citrin, The role of radiation therapy in the management of sarcomas, Surg. Clin. N. Am. 88 (2008) 629–646 (viii).

[5] B. Zhu, J.K. Davie, New insights into signalling-pathway alterations in rhabdomyosarcoma, Br. J. Canc. 112 (2015) 227–231.

[6] J.F. Shern, L. Chen, J. Chmielecki, J.S. Wei, R. Patidar, M. Rosenberg, L. Ambrogio, D. Auclair, J. Wang, Y.K. Song, C. Tolman, L. Hurd, H. Liao, S. Zhang, D. Bogen, A.S. Brohl, S. Sindiri, D. Catchpoole, T. Badgett, G. Getz, J. Mora, J.R. Anderson, S.X. Skapek, F.G. Barr, M. Meyerson, D.S. Hawkins, J. Khan, Comprehensive genomic analysis of rhabdomyosarcoma reveals a landscape of alterations affecting a common genetic axis in fusion-positive and fusion-negative tumors, Cancer Discov. 4 (2014) 216–231.

[7] M. Seki, R. Nishimura, K. Yoshida, T. Shimamura, Y. Shiraishi, Y. Sato, M. Kato, K. Chiba, H. Tanaka, N. Hoshino, G. Nagae, Y. Shiozawa, Y. Okuno, H. Hosoi, Y. Tanaka, H. Okita, M. Miyachi, R. Souzaki, T. Taguchi, K. Koh, R. Hanada, K. Kato, Y. Nomura, M. Akiyama, A. Oka, T. Igarashi, S. Miyano, H. Aburatani, Y. Hayashi, S. Ogawa, J. Takita, Integrated genetic and epigenetic analysis defines novel molecular subgroups in rhabdomyosarcoma, Nat. Commun. 3 (2015) 7557.

[8] E. Seto, M. Yoshida, Erasers of histone acetylation: the histone deacetylase enzymes, Cold Spring Harb Perspect Biol 6 (2014) a018713.

[9] S. Ropero, M. Esteller, The role of histone deacetylases (HDACs) in human cancer, Mol Oncol 1 (2007) 19–25.

[10] Y. Li, E. Seto, HDACs and HDAC inhibitors in cancer development and therapy, Cold Spring Harb Perspect Med 6 (2016) pii: a026831.

[11] E. Hedrick, L. Crose, C.M. Linardic, S. Safe, Histone deacetylase inhibitors inhibit rhabdomyosarcoma by reactive oxygen species-dependent targeting of specificity protein transcription factors, Mol. Cancer Ther. 14 (2015) 2143–2153.

[12] S.E. Ghayad, G. Rammal, O. Sarkis, H. Basma, F. Ghamloush, A. Fahs, M. Karam, M. Harajli, W. Rabeh, J.E. Mouawad, H. Zalzali, R. Saab, The histone deacetylase inhibitor Suberoylanilide Hydroxamic Acid (SAHA) as a therapeutic agent in rhabdomyosarcoma, Cancer Biol. Ther. 20 (2019) 272–283.

[13] B. Groselj, N.L. Sharma, F.C. Hamdy, M. Kerr, A.E. Kiltie, Histone deacetylase inhibitors as radiosensitisers: effects on DNA damage signalling and repair, Br. J. Canc. 108 (2013) 748–754.
[14] A.H.W. Nias, An Introduction to Radiobiology, John Wiley and Sons Ltd, Chichester, United Kingdom, 1998.
[15] K.K. Khanna, S.P. Jackson, DNA double-strand breaks: signaling, repair and the cancer connection, Nat. Genet. 27 (2001) 247–254.
[16] P.T. Schumacker, Reactive oxygen species in cancer: a dance with the devil, Cancer Cell 27 (2015) 156–157.
[17] F. Marampon, S. Codenotti, F. Megiorni, A. Del Fattore, S. Camero, G.L. Gravina, C. Festuccia, D. Musio, F. De Felice, V. Nardone, A.N. Santoro, C. Dominici, A. Fanzani, L. Pirtoli, A. Fioravanti, V. Tombolini, S. Cheleschi, P. Tini, NRF2 orchestrates the redox regulation induced by radiation therapy, sustaining embryonal and alveolar rhabdomyosarcoma cells radioresistance, J. Cancer Res. Clin. Oncol. 145 (2019) 881–893.
[18] C. Ciccarelli, F. Vulcano, L. Milazzo, G.L. Gravina, F. Marampon, G. Macioce, A. Giampaolo, V. Tombolini, V. Di Paolo, H.J. Hassan, B.M. Zani, Key role of MEK/ERK pathway in sustaining tumorigenicity and in vitro radioresistance of embryonal rhabdomyosarcoma stem-like cell population, Mol. Cancer 15 (2016) 16.
[19] F. Marampon, G.L. Gravina, A. Di Rocco, P. Bonfili, M. Di Staso, C. Fardella, L. Polidoro, C. Ciccarelli, C. Festuccia, V.M. Popov, R.G. Pestell, V. Tombolini, B.M. Zani, MEK/ERK inhibitor U0126 increases the radiosensitivity of rhabdomyosarcoma cells in vitro and in vivo by downregulating growth and DNA repair signals, Mol. Cancer Ther. 10 (2011) 159–168.
[20] F. Vulcano, C. Ciccarelli, G. Mattia, F. Marampon, M. Giampiero, L. Milazzo, M. Pascuccio, B.M. Zani, A. Giampaolo, H.J. Hassan, HDAC inhibition is associated to valproic acid induction of early megakaryocytic markers, Exp. Cell Res. 312 (2006) 1590–1597.
[21] G. Dobrowolny, E. Lepore, M. Martini, L. Barberi, A. Nunn, B.M. Scicchitano, A. Musarò, Metabolic changes associated with muscle expression of SOD1G93A, Front. Physiol. 9 (2018) 831.
[22] B.M. Scicchitano, S. Sorrentino, G. Proietti, G. Lama, G. Dobrowolny, A. Catizone, E. Binda, L.M. Larocca, G. Sica, Levetiracetam enhances the temozolomide effect on glioblastoma stem cell proliferation and apoptosis, Cancer Cell Int. 18 (2018) 136.
[23] G.L. Gravina, F. Marampon, I. Giusti, E. Carosa, S. Di Sante, E. Ricevuto, V. Dolo, V. Tombolini, E.A. Jannini, C. Festuccia, Differential effects of PXD101 (belinostat) on androgen-dependent and androgen-independent prostate cancer models, Int. J. Oncol. 40 (2012) 711–720.
[24] F. Dotiwala, J.C. Harrison, S. Jain, N. Sugawara, J.E. Haber, Mad2 prolongs DNA damage checkpoint arrest caused by a double-strand break via a centromere-dependent mechanism, Curr. Biol. 20 (2010) 328–332.
[25] P. Kaspar, J. Prochazka, M. Efenberkova, A. Juhasz, V. Novosadova, R. Sedlacek, c-Myb regulates tumorigenic potential of embryonal rhabdomyosarcoma cells, Sci. Rep. 9 (2019) 6342.
[26] S.R. Annavarapu, S. Cialfi, C. Dominici, G.K. Kokai, S. Uccini, S. Ceccarelli, H.P. McDowell, T.R. Helliwell, Characterization of Wnt/β-catenin signaling in rhabdomyosarcoma, Lab. Investig. 93 (2013) 1090–1099.
[27] K.K. Ganguly, S. Pal, S. Moulik, A. Chatterjee, Integrins and metastasis, Cell Adhes. Migrat. 7 (2013) 251–261.
[28] F. Marampon, G. Bossi, C. Ciccarelli, A. Di Rocco, A. Sacchi, R.G. Pestell, B.M. Zani, MEK/ERK inhibitor U0126 affects in vitro and in vivo growth of embryonal rhabdomyosarcoma, Mol. Cancer Ther. 8 (2009) 543–551.
[29] L. Cen, F.C. Hsieh, H.J. Lin, C.S. Chen, S.J. Qualman, J. Lin, PDK-1/AKT pathway as a novel therapeutic target in rhabdomyosarcoma cells using OSU-03012 compound, Br. J. Canc. 97 (2007) 785–791.
[30] C.V. Dang, K.A. O'donnell, T. Juopperi, The great MYC escape in tumorigenesis, Cancer Cell 8 (2005) 177–178.
[31] F. Marampon, C. Ciccarelli, B.M. Zani, Down-regulation of c-Myc following MEK/ERK inhibition halts the expression of malignant phenotype in rhabdomyosarcoma and in non muscle-derived human tumors, Mol. Cancer 5 (2006) 31.
[32] Y. Hachitanda, S. Toyoshima, K. Akazawa, M. Tsuneyoshi, N-myc gene amplification in rhabdomyosarcoma detected by fluorescence in situ hybridization: its correlation with histologic features, Mod. Pathol. 11 (1998) 1222–1227.
[33] L.J. Kuo, L.X. Yang, Gamma-H2AX - a novel biomarker for DNA double-strand breaks, Vivo (Brooklyn) 22 (2008) 305–309.
[34] G. Iliakis, Y. Wang, J. Guan, H. Wang, DNA damage checkpoint control in cells exposed to ionizing radiation, Oncogene 22 (2003) 5834–5847.
[35] J. Bartek, J. Lukas, Chk1 and Chk2 kinases in checkpoint control and cancer, Cancer Cell 3 (2003) 421–429.
[36] Y. Huang, R.M. Sramkoski, J.W. Jacobberger, The kinetics of G2 and M transitions regulated by B cyclins, PLoS One 8 (2013) e80861.
[37] E.R. Ballister, M.A. Lampson, Chromosomal instability: mad2 beyond the spindle checkpoint, Curr. Biol. 22 (2012) R233–R235.
[38] L. Michel, R. Benezra, E. Diaz-Rodriguez, MAD2 dependent mitotic checkpoint defects in tumorigenesis and tumor cell death: a double edged sword, Cell Cycle 3 (2004) 990–992.
[39] Y. Nakano, T. Sumi, M. Teramae, M. Morishita, T. Fukuda, H. Terada, H. Yoshida, Y. Matsumoto, T. Yasui, O. Ishiko, Expression of the mitotic-arrest deficiency 2 is associated with chemotherapy resistance in ovarian serous adenocarcinoma, Oncol. Rep. 28 (2012) 1200–1204.
[40] H.A. Cocker, C.R. Pinkerton, L.R. Kelland, Characterization and modulation of drug resistance of human paediatric rhabdomyosarcoma cell lines, Br. J. Canc. 83 (2000) 338–345.
[41] S. Elmore, Apoptosis: a review of programmed cell death, Toxicol. Pathol. 35 (2007) 495–516.
[42] Z. Herceg, Z.Q. Wang, Failure of poly(ADP-ribose) polymerase cleavage by caspases leads to induction of necrosis and enhanced apoptosis, Mol. Cell. Biol. 19 (1999) 5124–5133.
[43] V. Moresi, N. Marroncelli, D. Coletti, S. Adamo, Regulation of skeletal muscle development and homeostasis by gene imprinting, histone acetylation and microRNA, Biochim. Biophys. Acta 1849 (2015) 309–316.
[44] F. Marampon, C. Ciccarelli, B.M. Zani, Biological rationale for targeting MEK/ERK pathways in anti-cancer therapy and to potentiate tumour responses to radiation, Int. J. Mol. Sci. 23 (2019) 20.
[45] P. Zhang, C. Wong, D. Liu, M. Finegold, J.W. Harper, S.J. Elledge, p21(CIP1) and p57(KIP2) control muscle differentiation at the myogenin step, Genes Dev. 13 (1999) 213–224.
[46] G. Messina, C. Blasi, S.A. La Rocca, M. Pompili, A. Calconi, M. Grossi, p27Kip1 acts downstream of N-cadherin-mediated cell adhesion to promote myogenesis beyond cell cycle regulation, Mol. Biol. Cell 16 (2005) 1469–1480.
[47] S. Rossi, E. Stoppani, P.L. Puri, A. Fanzani, Differentiation of human rhabdomyosarcoma RD cells is regulated by reciprocal, functional interactions between myostatin, p38 and extracellular regulated kinase signalling pathways, Eur. J. Cancer 47 (2011) 1095–1105.
[48] L.V.1 Nguyen, R. Vanner, P. Dirks, C.J. Eaves, Cancer stem cells: an evolving concept, Nat. Rev. Cancer 12 (2012) 133–143.
[49] H. de Thé, Differentiation therapy revisited, Nat. Rev. Cancer 18 (2018) 117–127.
[50] G. Luther, R. Rames, E.R. Wagner, G. Zhu, Q. Luo, Y. Bi, S.H. Kim, J.L. Gao, E. Huang, K. Yang, L. Wang, X. Liu, M. Li, N. Hu, Y. Su, X. Luo, L. Chen, J. Luo, R. C Haydon, H.H. Luu, L. Zhou, T.C. He, Molecular basis of differentiation therapy for soft tissue sarcomas, Trends Cancer Res. 6 (2010) 69–90.
[51] Barnum KJ1, M.J. O'Connell, Cell cycle regulation by checkpoints, Methods Mol. Biol. 1170 (2014) 29–40.
[52] M.D. Garrett, I. Collins, Anticancer therapy with checkpoint inhibitors: what, where and when? Trends. Pharm. Sci. 32 (2011) 308–316.
[53] M. M Mc Gee MM, Targeting the mitotic catastrophe signaling pathway in cancer, Mediat. Inflamm. (2015) 146282 2015.